Adv. Radio Sci., 13, 49–55, 2015
www.adv-radio-sci.net/13/49/2015/
doi:10.5194/ars-13-49-2015


Advances in Radio Science
Open Access Proceedings

# Comparison of electromagnetic solvers for antennas mounted on vehicles

**M. S. L. Mocker[1], S. Hipp[2], F. Spinnler[1], H. Tazi[3], and T. F. Eibert[1]**

[1]Technische Universität München, Lehrstuhl für Hochfrequenztechnik, Arcisstrasse 21, 80333 Munich, Germany
[2]CST AG, Bad Nauheimer Str. 19, 64289 Darmstadt, Germany
[3]Audi AG, August-Horch Str., 85055 Ingolstadt, Germany

*Correspondence to:* M. S. L. Mocker (marina.mocker@tum.de)

Received: 26 December 2014 – Revised: 11 April 2015 – Accepted: 19 May 2015 – Published: 3 November 2015

**Abstract.** An electromagnetic solver comparison for various use cases of antennas mounted on vehicles is presented. For this purpose, several modeling approaches, called transient, frequency and integral solver, including the features fast resonant method and autoregressive filter, offered by CST MWS, are investigated. The solvers and methods are compared for a roof antenna itself, a simplified vehicle, a roof including a panorama window and a combination of antenna and vehicle. With these examples, the influence of different materials, data formats and parameters such as size and complexity are investigated. Also, the necessary configurations for the mesh and the solvers are described.

## 1 Introduction

For solving electromagnetic problems in complex environments, the choice of the most appropriate method does not only determine the time efficiency, but has an influence on the accuracy of the gained results, as well. There is not a single combination of a numerical method and algebraic solver, in the following called solver, which can fulfill all requirements. Moreover, many parameters, such as size in relation to wavelength, complexity and resonating behavior must be considered. In the following, the transient (T), the frequency (F) and the integral (I) solver offered in CST MWS (Weiland, 1996), (CST, 2015) are investigated.

The T solver is based on the finite integration technique. The geometrical model is here divided into hexahedra (Yee, 1966) and a time signal is propagated through the structure (Weiland, 2008). In general the hexahedral mesh is a very robust way of meshing for complicated structures, but has some disadvantages, for example in case of curved geometries. In these cases, the mesh must either be extremely dense or is meshed by utilizing the perfect boundary approximation technique, where sub-cellular information is taken into account for curved elements (Krietenstein, 2001). An improved mesh can be achieved by subgridding (Podebrad, 2003), where critical areas are meshed with more lines than the rest. For highly resonant structures such as antennas, the simulation duration may be very high or resonances may even not be simulated correctly at all due to an insufficient decay of energy within the system. This can be solved by an autoregressive (AR) filter (Percival, 1993) which drastically reduces the simulation time as the spectral properties can be retrieved from rather few time steps.

The F solver uses the finite element method. A limit for this method is the availability of random access memory (RAM) which is used mainly dependent on the number of mesh cells. The resulting matrix is sparsely populated as elements are only non-zero if nodes in the discretized geometry are neighboring. The numerical system size can be reduced by a model order reduction technique (MOR) (Ilic, 2004). In a first step, the structure is meshed with surface triangles and only in case there is a thickness, the volume is meshed with tetrahedra. At critical points, the mesh is corrected for the highest simulation frequency usually mainly by further refinements (Cendes, 1985; Pinchuk, 1985).

The I solver uses the Method of Moments. As only the surface must be meshed, the method is well suitable for large solution domains. Dielectrics are not meshed for this solver method in CST MWS.

In the following, the mentioned solvers and methods are investigated in order to simulate a complex roof antenna

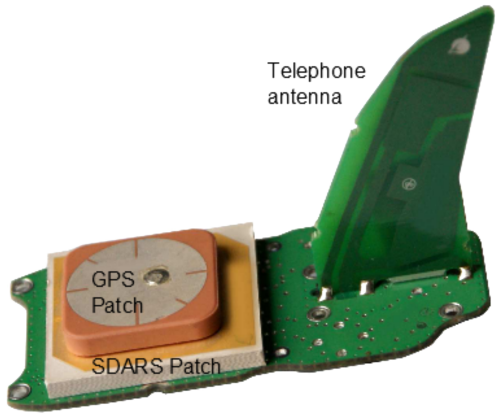


**Figure 1.** Photograph of the antenna structures.

**Figure 2.** Photograph of the antenna plastic cap.

**Table 1.** Services joined within one antenna assembly.

| Antenna | *S* Parameter | Frequencies |
|---|---|---|
| SDARS patch | $S_{11}$ | 2.33 GHz |
| GPS patch | $S_{22}$ | 1.58 GHz |
| Telephone fin | $S_{33}$ | 824–894 MHz |
| | | 1.85–1.99 GHz |
| | | 1.71–1.755 GHz |

mounted on a vehicle accurately and efficiently. Therefore, several simulations with the roof antenna itself are conducted. In a second step, the solvers are compared for the purpose of simulating extended simulation domains as vehicles and roofs. In these models, monopoles are used as simplified antennas in order to isolate the problems from each other. Finally, a vehicle including the roof antenna is simulated. Also, the influence of data formats and materials is taken into consideration. The values of interest for the feasibility and efficiency of a simulation are majorly the RAM and time consumption. Especially the time consumption is only a rough value. The benchmark computer has 2 processors of the type Intel(R) Xeon(R) CPU with E5640@2.67 GHz and 24 GB RAM. Each of the processors consists of 4 cores and moreover the Intel(R) Hyper-Threading Technology is enabled. Some simulations could not be performed on this computer so the necessary time was estimated. Simulations for the purpose of time comparability were started in order to estimate the differences in computation speed. Finally, the given times can be seen as benchmarks.

## 2 Roof antenna

The first part of the investigation is a roof antenna itself. The antenna designed for the north American market consists of a SDARS patch, a GPS patch and a telephone antenna, which are contained in one antenna assembly as shown in Fig.1. It is built by thin metal sheets and several dielectrics. All covered services are listed in Table 1. The antenna assembly is adapted to a mounting consisting of metal and plastic for the purpose of sealing and is covered by a housing of plastic as shown in Fig. 2.

All solvers explained above, except the I solver, are evaluated for the antenna model and finally compared to measurement results. All connections are modeled as coaxial structures. The antenna needs to be slightly modified for each solver. For the transient solver all ports were implemented as perfect conducting wires between two points realizing a source, called edge ports, whereas with the frequency solver a face is used instead of a thin wire, called discrete face ports, were used. This port modification does not relevantly change the simulation behavior as the results for the Global Positioning System (GPS) and Satellite Digital Audio Radio Services (SDARS) antennas do correspond well to each other. For the simulations with the T solver, the antenna is meshed using hexahedra as shown in Fig. 3. To ensure that all metalizations are correctly identified in the hexahedral mesh they are thickened in order to ensure at least 2 mesh lines for each material, even though this was only mandatory for dielectrics. For the F solver, the antenna is meshed with tetrahedra as shown in Fig. 4. The automatic discretization process is more stable for the hexahedral mesh in comparison to the tetrahedral mesh, especially if the model contains material jumps in combination with complicated structures.

The simulated and measured reflection parameters of the SDARS antenna are shown in Fig. 5 and of the telephone antenna in Fig. 6. The resonance frequencies are well met for the SDARS and GPS simulations and roughly for the simulation of the telephone antenna. In Table  the RAM and time consumption are listed for all simulations. Efficient and accurate simulations are possible with the F solver. After simplifications of the model by neglecting details and a manual optimization of the mesh by assigning discretization densities to different materials in the model, the number of cells can be reduced to 200 000 cells (Mocker, 2014). With the adaptive mesh, the results are not completely correct for resonance frequencies as shown in Fig. 6. The adaptive mesh of the F solver does not change the results of the SDARS and the

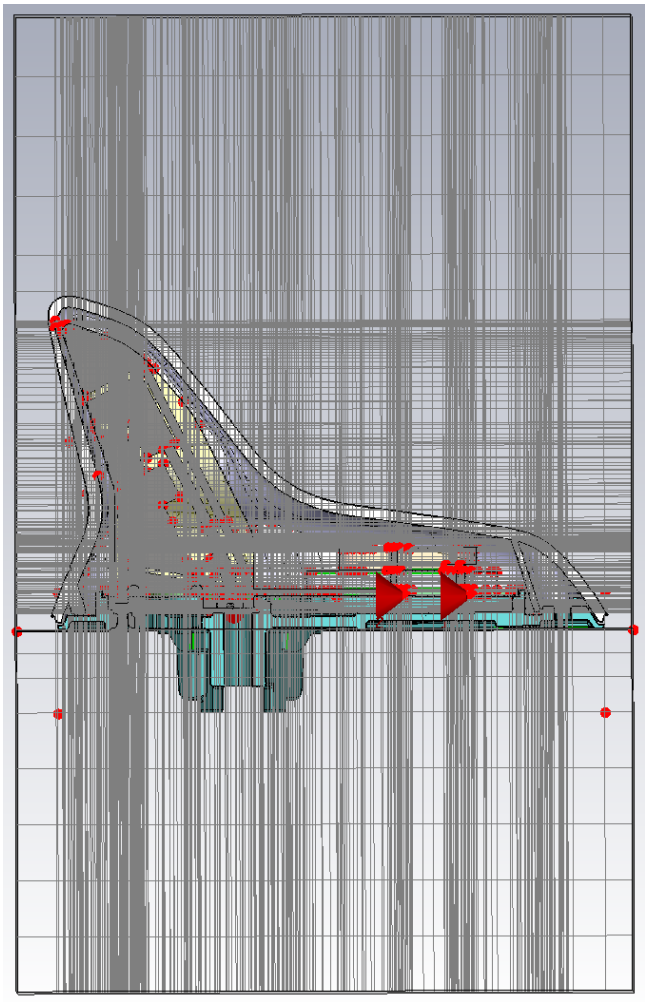

**Figure 3.** Hexahedral mesh.

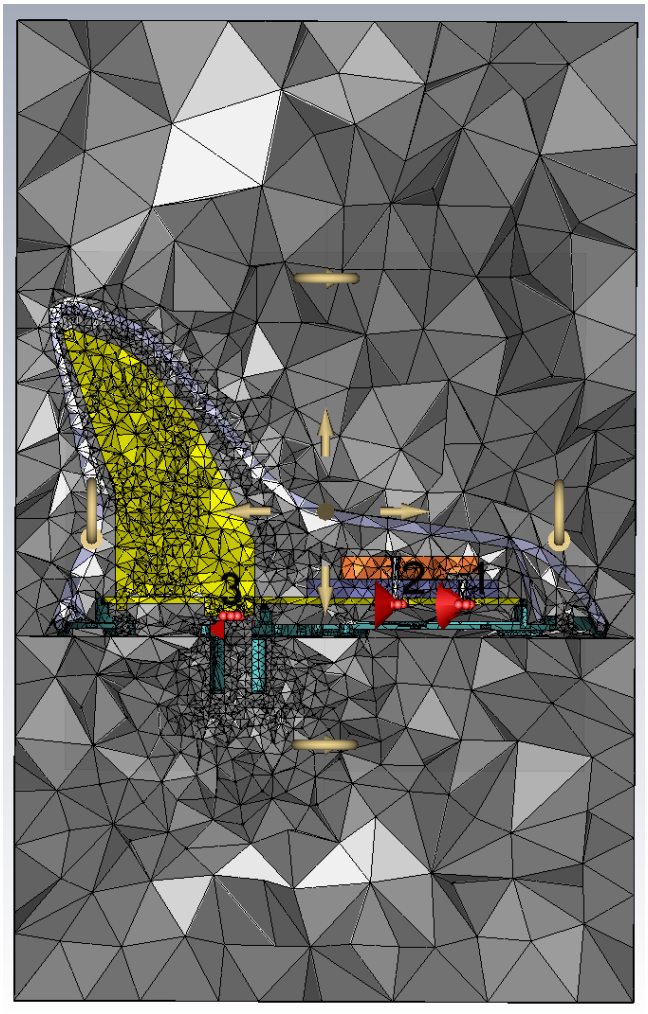

**Figure 4.** Tetrahedral mesh.

GPS antenna, but for the telephone antenna. For the frequencies over 1.5 GHz the reflection parameters change by using the adaptive mesh. If the simulation bandwidth is reduced, the newly arising resonances do not exist. A reason for this is that adaptive meshing algorithms in time and frequency domain analyze the simulated structure to increase the mesh density at high field values in order to decrease the simulation error. While in time domain the time pulse transports the energy, yielding a broadband adaption of the mesh, the frequency solver solves the equations at distinct frequency points and thus adapts at single frequency values. By default the highest possible frequency is used in order to assure the best resolution. However, maximum field values might occur at other points in the structure, namely where resonances take place. In order to account for this effect, it is possible to set the adaption to the resonances explicitly. If this option is not chosen, simulation results may differ for varying frequency bands due to different maximum frequencies. Using the resonant fast *S* Parameter method based on MOR does not relevantly improve the scattering parameters or the time consumption, but drastically increases the maximum RAM consumption. The MOR in this case is very costly so that the advantages do not carry weight. In all cases the resonances are more distinct in the simulations with the F solver, than with the T solver, because the energy only decays very slowly when propagating through the structure at the appearance of resonances. The standard configuration is to abort the simulation after a time according to 20 times the length of the input impulse. At this point of time the energy only decays to $\approx -40$ dB and ripples still exist in the scattering parameters. As well the adaptive mesh refinement cannot be used under these conditions as first results are necessary for the refinement of the mesh. A way to circumvent this problem is the AR Filter. With the AR Filter, the resonances can be estimated before the energy is decayed completely, thus, the simulation duration is reduced to less than one hour. The number of required adaptive mesh refinements cannot be given in general as it is dependent on the initial mesh.

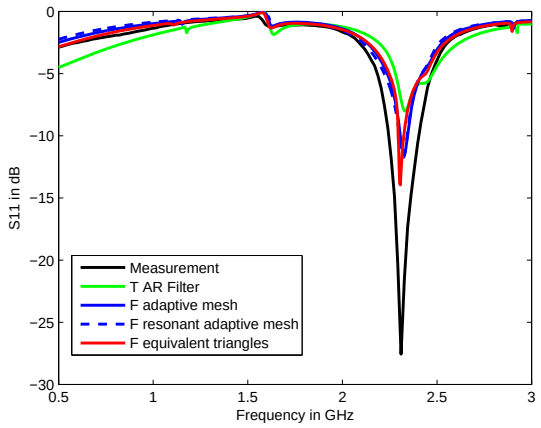


**Figure 5.** $S_{11}$ of the SDARS patch simulated with different solvers.

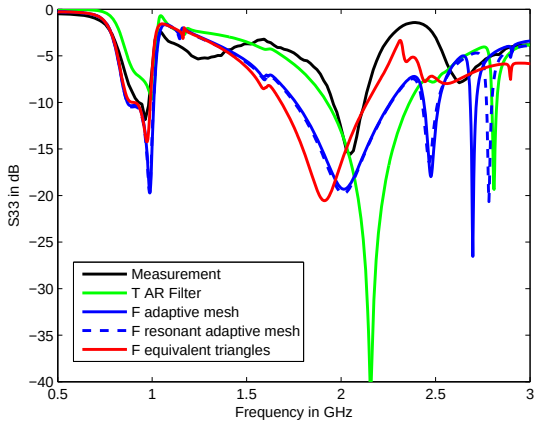


**Figure 6.** $S_{33}$ of the telephone antenna simulated with different solvers.

For useful investigations with the T solver, the AR filter is necessary. Once some experience with the meshing of the structure could be achieved, the most efficient simulations still can be undertaken with the F solver. A further advantage of the F solver is the fact that single frequencies can be simulated at frequency points of interest after the solver run has finished without performing adaptive meshing.

## 3 Extended simulation domains

Vehicles feature an extended and at the same time complex environment which strongly influences the far field patterns of roof antennas. A common data format for vehicles is the Computer Aided Three-Dimensional Interactive Application (CATIA) format. In this format, every detail is included and the total amount of data is by far too extensive for the import into electromagnetic field solver programs. To reduce the amount of data and for reasons of compatibility the data is simplified to Nasa Structural Analysis System (NASTRAN) data, in which the surface is represented by triangles

**Table 2.** Comparison of different solver for the roof antenna.

| Solver | F | F | F | T |
|---|---|---|---|---|
| Configuration | – | – | MOR (res) | AR |
| Mesh | Optimized | Adaptive | Adaptive | one cycle |
| Elements | 200 000 | 370 000 | 267 982 | 6 373 600 |
| RAM | 2.7 GB | 4.6 GB | 27 GB | 4.6 GB |
| Time ≈ | 2 h | 4 h, 15 min | 1 h, 21 min | 49 min |

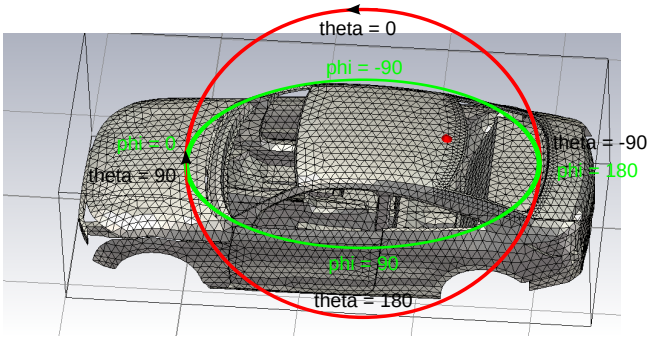


**Figure 7.** Nastran mesh of a vehicle.

as shown in Fig. 7. For the investigation of the efficiency and the accuracy of the solvers, the antenna is simplified to a monopole which is located in the rear part of the roof.

The simulation with the T solver is carried out in a frequency range from 1 to 2.5 GHz and the impulse is propagated through the structure until the energy level decreased to −30 dB. The mesh configuration is 10 lines per wavelength with a mesh line ratio limit of 999, which indicates the ratio of the largest cell size to the smallest cell size. The adaptive mesh refinement is an automatic refinement process in order to improve the mesh quality, especially in areas with high levels of electromagnetic energy the discretization is refined. It is deactivated in the simulations described in the following, as each refinement step approximately takes as long as the simulation duration given in Table 3. The simulation with the I solver is carried out for one single frequency point at 2 GHz. The I solver is configured with first solver order, an accuracy of 0.001 and 10 and 5 mesh cells per wavelength $\lambda$ are used. The F solver meshing is configured with the default values allowing curved elements. The far field patterns simulated with all solvers are approximately similar as shown in Fig. 8. The comparability of the RAM and time consumption in Table 3 is only possible taking into consideration the varying frequency bandwidth and maximum frequency. The T solver is simulated in a broad frequency bandwidth with a maximum frequency of 2.5 GHz whereas the I and F solver are started at one single frequency point at 2 GHz. The decreased maximum frequency means that there are less mesh cells necessary in total.

The time efficiency of the solvers is dependent on the number of frequencies of interest. In case only one frequency

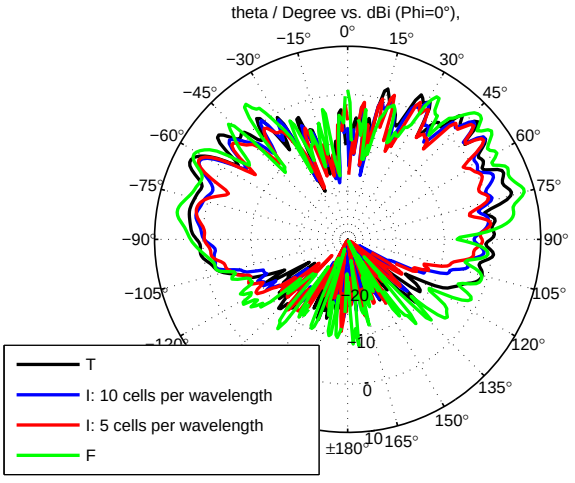


**Figure 8.** Far field simulation results at 2 GHz for T, F and I solver with different accuracies.

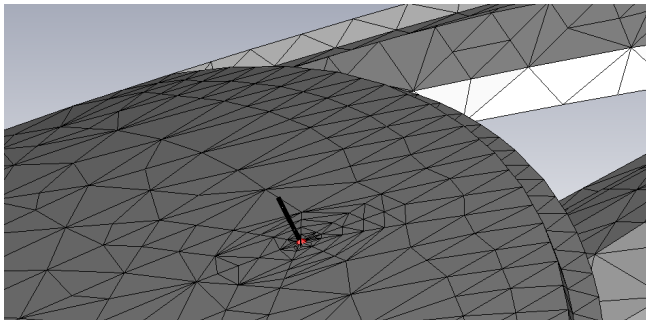

**Figure 9.** Meshing of NASTRAN structure with triangles.

point is investigated, the I solver is faster than the T solver. As soon as scattering parameters should be simulated at the same time, a larger bandwidth is necessary for reasonable investigations and the time consumption with the I solver will increase. Additionally it must be considered that windows are important for the far field behavior which were not considered in the I solver as they are dielectrics.

For the I and F solver a reduction of the overall model by deleting parts which do not influence the far field patterns, brings advantages as there are less triangles. With the T solver this effect is less distinctive because the whole box including air is meshed. For this reason, in the following only the roof is taken into consideration. Another vehicle model had to be used for the roof comparisons. Usually vehicle models are prepared in NASTRAN format at AUDI AG. The disadvantage of the NASTRAN format in CST MWS is that the mesh gets unnecessary fine as the triangles cannot be loaded as the mesh itself but are meshed a second time as shown in Fig. 9. Even if the triangles could be loaded as the final mesh, the limitation to a specific frequency by the size of the triangles makes this process inflexible. Originally,

**Table 3.** Comparison of different solvers for the monopole on a metallic vehicle modeled in NASTRAN.

| Solver | T | I (10 cells/λ) | I (5 cells/λ) | F |
|---|---|---|---|---|
| Frequency | 1–2.5 GHz | 2 GHz | 2 GHz | 2 GHz |
| Elements | 48 341 870 | 278 649 | 75 000 | 496 000 |
| RAM | 6.6 GB | 5.1 GB | 1.7 GB | 19.3 GB |
| Time ≈ | 10 h, 40 min | 2 h, 40 min | 2 h, 20 min | 20 min |

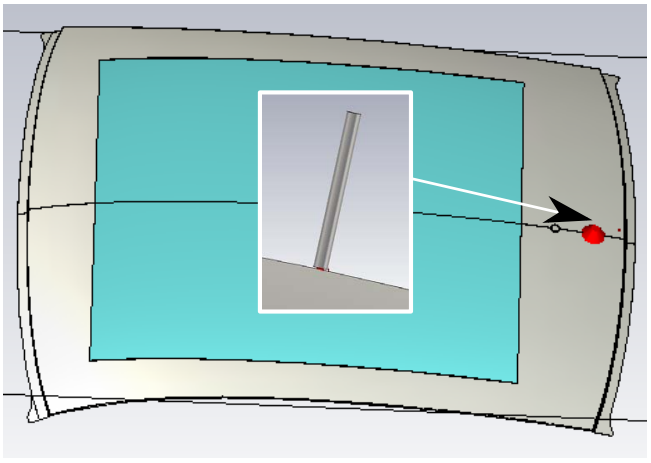

**Figure 10.** Roof with panorama glass window and monopole as simplification of an antenna.

the vehicles are saved in CATIA format which represents the geometry as non-uniform rational basis splines (NURBS).

In Table 4, the comparison of a metallic roof imported in NASTRAN and CATIA format is shown. With the CATIA format, reasonable results could be gained in the T solver with a mesh configuration of 10 lines per λ, whereas the NASTRAN format needs 3 times more mesh cells to meet the resonance frequency and the expected far field. At points, where the structure is discontinuous or at the end of straight lines describing the surface, the automatic meshing detects fixpoints, where discretization lines are applied. It is important to switch off the fixpoints as the hexahedral mesh would be by far too dense to even start the solver. Still some fixpoints around the antenna and the port are necessary. The mesh configuration was set equal to the configuration giving good results for the CATIA model. Within 3 cycles of adaptive mesh refinement the configuration was changed to 34 lines per λ. The first cycle takes 5 h, the second cycle 8 h and the third cycle, finally giving the expected resonance frequency of the monopole takes 10 h. In case the mesh configurations are known, the adaptive mesh can be skipped and the values as given in Table 4 can be expected. Another disadvantage of the NASTRAN format is the thickening of the triangular surface in order to prepare the model for the meshing with hexahedra. The far field pattern in vertical cut is shown in Fig. 12.

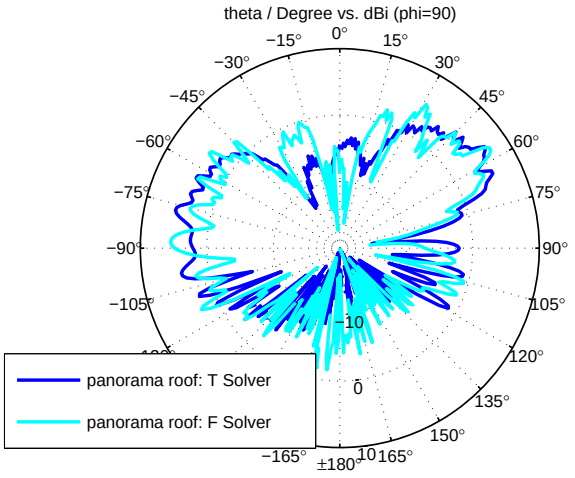


**Figure 11.** Far field patterns at 2 GHz simulated with T and with F solver.

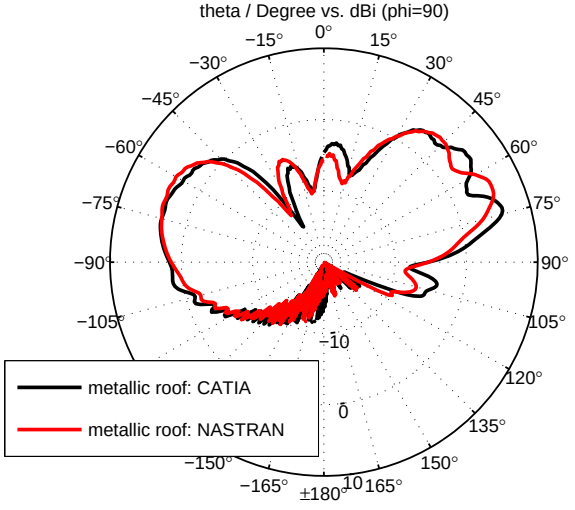


**Figure 12.** Simulated far field results at 2 GHz comparing the simulation using a roof model in CATIA and NASTRAN format.

The differences between the two plots can be explained by the deviations of the models which result from the conversion to NASTRAN. The problem changes when dielectrics as glass are introduced. For that a rectangular glass window is introduced into the roof as shown in Fig. 10. The vehicle roof with and without glass is investigated with the T solver. The simulations were carried out for a frequency range from 1 to 6.5 GHz. The metallic roof has a size of approximately 1.35 m × 1.15 m. The introduced window has a size of 1 m × 0.9 m which means that approximately 60 % are then consisting of glass. The wavelength $\lambda$ in glass, with an $\epsilon_r$ equal to 7, for the highest simulated frequency of 6.5 GHz is 17.4 mm. In free space the wavelength is 46 mm. This explains the increased number of mesh cells as shown in Table 4 which also leads to an increase of RAM and time consumption. The dramatic increase of time consumption in the simulation with the panorama glass window can be explained by the fact that data was swapped from the RAM to the hard disk, as only 12 GB of RAM were available.

**Table 4.** Comparison of different solvers for the monopole on a roof and influence of a panorama glass window.

| Solver | T | T | T | F |
|---|---|---|---|---|
| Data Format | NASTRAN | CATIA | CATIA | CATIA |
| Material | Metal | Metal | Panorama | Panorama |
| Surface | Sheet | Volume | Volume | Volume |
| Elements | 99 059 100 | 33 885 108 | 51 251 112 | 1 591 851 |
| RAM | 11.7 GB | 7.7 GB | 11.6 GB | 73 GB |
| Time ≈ | 10 h | 15 h | 50 h | 20 h |

The results of the simulated far field patterns correspond to typically observed results. A typical effect with panorama windows is the damping of the far field in the horizontal direction (Kwoczek, 2011). This effect is only observable in the simulation in case the glass has a sufficient thickness which was in this case set to approximately 4 mm in order to guide the wave through the glass. The CATIA model with the panorama window was additionally simulated with the F solver. The frequency in this simulation ranges from 1 to 6.5 GHz which is the same range as with the simulations with the T solver. There are some deviations between the simulations with the T and the F solver. The reflection parameters with the F solver shows a more broadband resonance and the far field at 2 GHz shown in Fig. 11 also shows some deviations. Overall the results of the T solver are more credible. The F solver is faster, but still needs more RAM.

## 4 Roof antenna on vehicle

The far field pattern is, in contrast to the scattering parameters, not only dependent on a small area around the antenna. This is why a simulation of the model including the vehicle from Fig. 7 and the roof antenna from Fig. 4 and Fig. 3 is necessary. The previous investigations and comparisons of the different solvers show that only the T solver can perform this simulation and high-performance computers are required. So the simulation is conducted on a workstation with 4 Tesla K40 graphic processing units (GPU) (NVIDIA, 2014). For the meshing, 10 lines per $\lambda$, a lower mesh limit of 10 and a mesh line ratio limit of 600 is used. To ensure that the antenna is meshed in the same way as before fixpoints were used. Still they must be ignored for the vehicle in NASTRAN format. These configurations lead to 513 218 568 mesh cells in total. The accuracy is set to −30 dB.

With these settings the same reflection parameters as with the T solver in Figs. 5 and 6 are achieved. For the simulation 61 GB of RAM and an adaptive meshing is necessary with 3 cycles each taking 27 to 43 h. Altogether the simulation duration aggregates to 118 h.

## 5 Conclusions

In this paper, the theoretical background of the F, T and I solver and their accuracy and efficiency for a roof antenna mounted on a vehicle were discussed. The results show that the choice of the solver is not only dependent on the structure of the simulation domain, but also on the demanded results. The scattering parameters are more dependent on the structure itself, whilst the far field is strongly dependent on the environment. For the simulation of the roof antenna itself the T solver under usage of the AR filter and the F solver give good results whereas the vehicle is most efficiently simulated using the T solver, especially in case it contains dielectrics as glass. For this reason, the roof antenna including the vehicle was simulated with the T solver using the AR filter. The meshing of both the vehicle and the antenna works out the best when importing the data in CATIA format. The scattering parameters were validated with measurements and the far field patterns agreed with experiences from similar measurements. By comparing the different ways of simulations, an efficient way for investigating further antenna systems concerning scattering parameters as well as far field patterns could be described.

*Acknowledgements.* The authors wish to thank AUDI AG for providing CAD Data which are used in the simulation models and for the measurement data which serve to validate the simulation results. Also, a special thanks goes to the company CST AG for parts of the investigations and the simulation support.

Edited by: R. Schuhmann
Reviewed by: S. Lindenmeier and one anonymous referee

## References

Cendes, Z. J. and Shenton, D. N.: Adaptive Mesh Refinement in the Finite Element Computation of Magnetic Fields, IEEE Transactions on Magnetics, vol. MAG-21, 1811–1816, September 1985.

CST Computer Simulation Technology AG: CST MWS Description, available at: https://www.cst.com/Products/CSTMWS (last access: November 2014), 2015.

Ilic, M. M., Ilic, A. Z., and Notaros, B. M.: Higher Order Large-Domain FEM Modeling of 3-D Multiport Waveguide Structures With Arbitrary Discontinuities, IEEE Trans. Microw. Theory Tech., 52, 1608–1614, 2004.

Krietenstein, B., Schuhmann, R., Thoma, P., and Weiland, T.: The perfect boundary approximation technique facing the big challenge of high precision field computation, 19th International Linear Accelerator Conference, 2001.

Kwoczek, A., Raida, Z., Lacik, J., Pokorny, M., Puskely, J., and Vagner, P.: Influence of car panorama glass roof antenna on car2car communication, Vehicular Networking Conference, 2011.

Mocker, M. S. L., Engelmann, S., Tazi, H., and Eibert, T. F.: Finite Element Model Generation for Efficient and Accurate Electromagnetic Vehicle Roof Antenna Simulations, Loughborough Antennas and Propagation Conference, November 2014.

NVIDIA GmbH: Tesla K40 GPU, available at: http://www.nvidia.com/object/tesla-servers.html, last access: November 2014.

Percival, D. B. and Walden, A. T.: Spectral Analysis for Physical Applications: Multitaper and Conventional Univariate Techniques, Cambridge University Press, 1st Edn., 1993.

Pinchuk, A. R. and Silvester, P. P.: Error Estimation for Automatic Adaptive Finite Element Mesh Generation, IEEE Trans. Magnetics, MAG-21, 2551–2554, 1985.

Podebrad, O., Clemens, M., and Weiland, T.: New Flexible Subgridding Scheme for the Finite Integration Technique, IEEE Trans. Magnetics, 39, 1662–1665, 2003.

Weiland, T.: Time Domain Electromagnetic Field Computation with Finite Difference Methods, Int. J. Numer. Model., 9, 295–319, 1996.

Weiland, T., Timm, M., and Munteanu, I.: A Practical Guide to 3-D Simulation, IEEE Microwave Maga., 62–75, 2008

Yee, K. S.: Numerical solution of initial boundary value problems involving maxwell's equations in isotropic media, IEEE Trans. Ant. Propagation, 15, 802–907, 1966,